2017

# Effect of groove spacing on bond strength of near-surface mounted (NSM) bonded joints with multiple FRP strips

Shi Shun Zhang
*University of Wollongong*, shishun@uow.edu.au

Tao Yu
*University of Wollongong*, taoy@uow.edu.au

# Effect of groove spacing on bond strength of near-surface mounted (NSM) bonded joints with multiple FRP strips


## Abstract

In the strengthening of existing deficient structures using the near-surface mounted (NSM) FRP method, a group of parallel NSM FRP strips are usually needed to meet the capacity enhancement requirement. When the groove spacing (i.e., the net distance between grooves) is relatively small, the bond behaviour of each NSM FRP strip is detrimentally influenced by the adjacent grooves/FRP strips, and such detrimental effect should be taken into account for a safe design of the NSM FRP strengthening system. All the existing models, however, have been proposed for NSM bonded joints with a single FRP strip and thus cannot consider the effect of groove spacing on the bond behaviour, due to the insufficiency of data from tests or numerical simulations. Against this background, a numerical parametric study, was conducted to clarify the effect of groove spacing on the bond strength of such bonded joints; the numerical parametric study involved the use of a three-dimensional meso-scale finite element model developed in the present study for NSM bonded joints with two FPP strips separately embedded in two parallel grooves. Based on the results from the parametric study, a reduction factor to account for the detrimental effect of insufficient groove spacing on the bond strength is proposed and extended to NSM bonded joints with three or more evenly-spaced FRP strips. By combining the proposed reduction factor and the bond strength model previously developed by the authors for NSM bonded joints with a single FRP strip, a bond strength model for NSM bonded joints with multiple FRP strips is proposed and the accuracy of the proposed model is verified with test results.



## Keywords

groove, effect, multiple, joints, bonded, (nsm), mounted, near-surface, strips, strength, frp, bond, spacing

## Disciplines

Engineering | Science and Technology Studies

## Publication Details

Zhang, S. S. & Yu, T. (2017). Effect of groove spacing on bond strength of near-surface mounted (NSM) bonded joints with multiple FRP strips. Construction and Building Materials, 155 102-113.

# Effect of Groove Spacing on Bond Strength of Near-Surface Mounted (NSM) Bonded Joints with Multiple FRP Strips

S.S. Zhang[1,*] and T. Yu[2]

**Abstract:** In the strengthening of existing deficient structures using the near-surface mounted (NSM) FRP method, a group of parallel NSM FRP strips are usually needed to meet the capacity enhancement requirement. When the groove spacing (i.e., the net distance between grooves) is relatively small, the bond behaviour of each NSM FRP strip is detrimentally influenced by the adjacent grooves/FRP strips, and such detrimental effect should be taken into account for a safe design of the NSM FRP strengthening system. All the existing models, however, have been proposed for NSM bonded joints with a single FRP strip and thus cannot consider the effect of groove spacing on the bond behaviour, due to the insufficiency of data from tests or numerical simulations. Against this background, a numerical parametric study, was conducted to clarify the effect of groove spacing on the bond strength of such bonded joints; the numerical parametric study involved the use of a three-dimensional meso-scale finite element model developed in the present study for NSM bonded joints with two FPP strips separately embedded in two parallel grooves. Based on the results from the parametric study, a reduction factor to account for the detrimental effect of insufficient groove spacing on the bond strength is proposed and extended to NSM bonded joints with three or more evenly-spaced FRP strips. By combining the proposed reduction factor and the bond strength model previously developed by the authors for NSM bonded joints with a single FRP strip, a bond strength model for NSM bonded joints with multiple FRP strips is proposed and the accuracy of the proposed model is verified with test results.

**Keywords:** concrete; fiber-reinforced polymer (FRP); strip; near-surface mounted (NSM); groove spacing; finite element (FE) model; bond strength model

[1]Lecturer, School of Civil, Mining and Environmental Engineering, Faculty of Engineering and Information Sciences, University of Wollongong, Wollongong, NSW 2522, Australia (corresponding author). E-mail address: shishun@uow.edu.au.

[2]Senior Lecturer, School of Civil, Mining and Environmental Engineering, Faculty of Engineering and Information Sciences, University of Wollongong, Wollongong, NSW 2522, Australia.

# 1 INTRODUCTION

The near-surface mounted (NSM) fiber-reinforced polymer (FRP) strengthening technique, as a promising alternative to the externally bonded (EB) FRP method for structural strengthening, has attracted worldwide attention over the last decade. Compared with the EB FRP method, the NSM FRP method has a number of advantages, including a higher bonding efficiency and a better protection of the FRP reinforcement [1]. FRP bars of various cross-sectional shapes (e.g. square, round and rectangular bars) have been studied by researcher as NSM FRP reinforcement. Existing experimental studies have showed that compared with other cross-sectional shapes, FRP strips (i.e., rectangular bars with a large aspect ratio) possesses a much better bonding efficiency (i.e., a higher local bond strength and a higher interfacial fracture energy), as they have a larger perimeter-to-cross-sectional area ratio and a larger embedment depth [e.g. 2-5]. In terms of material type, carbon FRP (CFRP) are thought to be more attractive than other types of FRP for the application of NSM strengthening technique, as CFRP usually has a higher strength and stiffness and thus could lead to a small cross-sectional area with the same demand in load-carrying capacity. Therefore, CFRP strips have become very popular for the use in NSM FRP strengthening and have attracted a large number of studies [e.g. 1, 5-7]. As one of the fundamental issues in the application of NSM FRP strengthening method, the bond strength, which is the maximum force that can be developed in the FRP reinforcement in the test of bonded joints [e.g. 8, 9], has been studied by a number of researchers, and several bond strength models have been proposed for NSM FRP-to-concrete interfaces by directly regressing test results on NSM FRP-to-concrete bonded joints [e.g. 10, 11] or conducting a numerical parametric study [e.g. 12, 13]. All the existing models, however, were proposed for a single FRP strip NSM to concrete and thus have not taken into account the effect of groove spacing (i.e., the net distance between grooves $a_g$, as shown in Fig. 1) on the bond behaviour. In real application of NSM FRP

strengthening method, including flexural strengthening and shear strengthening of RC members, a group of parallel NSM FRP strips (as shown in Fig. 1) need to be applied to meet the capacity enhancement requirement, and their bond behaviour may be detrimentally influenced by the adjacent grooves/FRP strips. The detrimental effect of insufficient groove spacing on the bond behaviour between NSM FRP reinforcement and concrete has not yet been clarified.

## 2 DETRIMENTAL EFFECT OF INSUFFICIENT GROOVE SPACING

When a group of two FRP strips (separately embedded in two parallel grooves) are used in the NSM strengthening method, the detrimental effect of insufficient groove spacing on the bond behaviour of each FRP strip only exists on the side where the adjacent FRP strip (referred to as adjacent FRP side for simplicity) is embedded. The bond behaviour on the other side (referred to as outer side for simplicity) is free from such detrimental effect, and thus the bond strength contributed from the outer side can be assumed to be half of the bond strength of NSM bonded joints with a single FRP strip. The difference between the total bond strength of each FRP strip and the bond strength contributed from the outer side is just the bond strength contributed from the adjacent FRP side. A reduction factor to account for such effect on the bond strength can therefore be obtained, i.e., the ratio between the bond strength from the adjacent FRP side and half of the bond strength of NSM bonded joints with a single FRP strip. This reduction factor can be extended to situations where a group of three or more FRP strips (embedded in evenly-spaced parallel grooves) are used. Among these FRP strips, each of the two outmost FRP strips suffers the detrimental effect of insufficient groove spacing from one side and thus the reduction factor only needs to be applied on one side in the calculation of the bond strength of each FRP strip, while each of the inner FRP strips suffers such detrimental effect from both sides and thus the reduction factor needs to be

applied on both sides in the calculation of the bond strength of each FRP strip.

Against the above background, a three-dimensional (3-D) meso-scale finite element (FE) model of bonded joints with two CFRP strips is developed, based on the FE model established by Teng *et al.* [14] for bonded joints with a single CFRP strip whose accuracy has been verified with experimental results. A numerical parametric study, covering the most important parameters, is conducted in the present paper by adopting the developed FE model. Based on the results of the parametric study, a reduction factor is proposed to account for the effect of groove spacing on the bond strength. By introducing the proposed reduction factor into the bond strength model previously proposed by the authors (Zhang *et al.* 2014) for bonded joints with a single FRP strip, a new bond strength model is established for bonded joints with multiple FRP strips. The performance of the new bond strength model is then assessed with the existing test results.

# 3 FINITE ELEMENT (FE) MODEL

## 3.1 General

Based on the 3-D meso-scale model developed by Teng *et al.* [14] for the single-lap shear test of NSM FRP strips-to-concrete bonded joints (referred to as NSM bonded joints hereafter for simplicity) with a single FRP strip, the FE model for NSM bonded joints with two FRP strips separately embedded in two parallel grooves (referred to as NSM bonded joints with two FPP strips hereafter for simplicity) was built in the present study, using the software package MSC.MARC [15]. It has been proved that the FE model established by Teng *et al.* [14] can well predict the failure process and ultimate load of NSM bonded joints with a single FRP strip, as well as the strain distributions of the FRP and the local bond-slip relationship between NSM FRP strip and concrete [14]. The failure mechanism of the current case is the same as that modelled in [14], with the only difference being that two FRP strips instead of

one need to be included in the built FE model. Failure of NSM bonded joints may happen in the materials (i.e., FRP, adhesive and concrete) or at FRP-to-adhesive/concrete-to-adhesive interfaces [13, 14]. However, it has been widely accepted that in practical applications, it should be guaranteed that the final failure is controlled by the failure in concrete as otherwise the strengthening efficiency cannot be maximized. Existing experimental studies, in fact, have proved that cohesive failure in concrete can be ensured by using an appropriate adhesive (usually with a tensile strength much higher than the concrete) and by carrying out appropriate surface preparation before application [13]. Therefore, in the numerical simulation of NSM bonded joints, the accurate modelling of concrete material is of critical importance. Following Teng *et al.* [14], the modelling of concrete, in particular the tensile and shear behavior of the cracked concrete, was carefully treated in the present study. The well-established tension-softening curve and the shear retention factor model for cracked concrete were incorporated into the FE model through user-defined subroutines.

### 3.2 FE model and boundary conditions

The schematic of the NSM bond joints with two parallel FRP strips modelled in the present study is shown in Fig. 2. The specimens have a height of 150 mm and a total length of 550 mm. The bond length of the FRP is 450mm, which is longer than the effective bond length according to Zhang *et al.* [13] and Seracino *et al.* [9]. A length of 75 mm is left near the loaded end to avoid local shear failure at loaded end, while a length of 25 mm is left near the free end of the FRP strip. The concrete edge distances (i.e., $a_e$ in Figs. 1 and 2, the distance between the outmost groove and the nearer edge of the concrete) in the specimen is changed according to the height of the FRP strip, which will be introduced in details later in the parametric study. Only half of the specimen is included in the FE model (Fig. 2), by taking advantage of symmetry. In addition, the bottom layer of concrete block with a height of 50 mm was not included in the FE model. Such simplification has only marginal effect on the

modeling accuracy but can significantly save the computational time [14]. The applied boundary conditions include (Fig. 2): (1) the displacements in the width direction of the specimen are prevented on the plane of symmetry; (2) the lower portion (with a height of 50 mm) of the vertical surface of the concrete block at the loaded end is restrained in the length direction of the specimen; and (3) the displacement of bottom surface of the concrete block in the vertical direction is restrained. First-order solid elements, which have eight nodes and full Gaussian integration scheme, are used to model the concrete block, the CFRP strip and the adhesive. Interfacial elements between NSM FRP and concrete are not necessary in the present study, as the 3-D meso-scale FE model is able to accurately capture the debonding process by using very small elements [14]. Following Teng *et al.* [14], very fine mesh with an element size in the order of 1 mm are employed in building the FE model.

### 3.3 Constitutive models

The orthogonal fixed smeared crack model, which is available in MSC.MARC [15], is used to model the cracked concrete. For orthogonal fixed smeared crack model, a maximum of three cracks could occur at each integration point, with their directions being orthogonal to each other. To eliminate the problem of mesh sensitivity, the crack band model proposed by Bazant and Oh [16] is adopted in the FE model, and the tensile fracture energy of cracked concrete given by CEB-FIP [17] is adopted. The yield law proposed by Buyukozturk [18] is used to describe the compression-dominated behaviour of concrete (with the associated flow rule), with the stress-strain behaviour being defined by the Elwi and Murray's [19] compressive stress-strain curve for concrete. The initiation of cracking is detected by the maximum tensile stress criterion. Hordijk's [20] exponential softening curve is used to model tension-softening behavior of cracked concrete, and Okamura and Maekawa's [21] model is used to describe the shear stress-slip behavior of cracked concrete. Both adhesive and FRP are assumed to be isotropic elastic materials. The simplification in the modelling of FRP and

adhesive was found to have nearly no effect in such simulation [14]. For more details of the adopted constitutive models, the readers are referred to Teng *et al.* [14] or Zhang and Teng [22, 23].

# 4 DESIGN OF PARAMETRIC STUDIES

## 4.1 Significance analysis of parameters

Before the above built FE model to be employed in the parametric study to investigate the effect of groove spacing on the bond strength, an analysis of the involved parameters should be carried out to identify the significant factors for the present study.

As the cohesion failure in the concrete near the epoxy-to-concrete interface is the failure mode of interest in the present study, the strength of concrete ( $f_c$ ) is obviously one of the most important parameter in determining the bond strength. A higher strength of concrete gives a higher fracture energy of concrete and thus a larger bond strength. The groove dimensions also have significantly effect on the bond behaviour: a deeper groove leads to a larger embedment depth of the FRP strip and thus a higher confinement from the surrounding concrete to the FRP strip can be expected. Therefore, the aspect ratio of the groove (i.e., the groove height $h_g$ to groove width $w_g$ ratio) should be important in determining the bond behavior and thus should be included in the parametric study. The thickness of the FRP strip is chosen to be 2 mm (a typical value for commercial CFRP strips), while the height of FRP strip varies in the parametric study to achieve various heights of the groove. The elastic modulus of the CFRP strip in the longitudinal direction is chosen to be 150 GPa (a typical value for pultruded CFRP strips).

As the adhesive was assumed to be linear-elastic material, the slip between FRP and concrete

under a certain local bond stress is only dependent on the thickness and the shear modulus of the adhesive layer. It has been reported by Zhang *et al.* [12] that for commonly used adhesives in NSM CFRP strengthening technique (with an elastic modulus not larger than 5 GPa), the adhesive thickness, which varies in the practical range (e.g. around 1-4 mm), has only marginal effect on the slip between the NSM FRP and concrete, as most slip is contributed by the concrete layer adjacent to the concrete-to-adhesive interface. In the present study, the elastic modulus and the thickness of adhesive are taken to be 3 GPa and 2 mm respectively (both are typical values in practice).

Existing studies have shown that the bond strength of NSM bonded joint increases with the bond length, until the bond length reaches a threshold value. The threshold value of the bond length has been commonly referred to as the effective bond length ( $L_e$ ) [8]. When the bond length is larger than the effective bond length, any further increase in the bond length does not lead to a further increase in the bond strength. In the present study, the bond length was chosen to be 450 mm, which is sufficiently large to eliminate its detrimental effect on the bond strength, based on Zhang *et al.* [13] and Seracino *et al.* [9]. Furthermore, the bond strength of an NSM bonded joint can be also affected by concrete edge distances (i.e., $a_e$ in Figs. 1 and 2). In the present study, to eliminate the detrimental effect of edge distance on the bond strength, sufficiently large values of concrete edge distance are chosen based on the height of FRP strip, according to Zhang *et al.* [12].

### 4.2 Numerical specimens in the parametric study

Based on the above considerations, the numerical specimens examined in the parametric study are designed and listed in Table 1. A total of 45 specimens are analyzed in the parametric study, with studied parameters covering the concrete strength, the height-to-width ratio of the groove, and groove spacing. Three values of the cylinder compressive strength of

concrete are used respectively: 20 MPa, 30 MPa and 40 MPa; three groove height-to-width ratios are considered respectively: 2.33, 4.00 and 5.67. The groove height-to-width ratios are achieved by changing the height of the grooves with the same width being used for all numerical specimens. The width of the groove is 6 mm, which is the summation of the thickness of CFRP strip (2mm) and the thickness of the adhesive layer (2mm on each side of the strip). The heights of the grooves are 14 mm, 24 mm and 34 mm respectively for CFRP strips with a height of 10 mm, 20 mm and 30 mm, as a 2mm-thick adhesive layer exists on the top as well as the bottom of the strip. The maximum value of 34 mm is chosen based on the consideration that the concrete cover thickness is not much larger than 35 mm in most practical cases, while the minimum value of 14 mm corresponds to FRP strips with a height-to-thickness ratio of 5, which is the lower bound for CFRP strips suggested by Zhang *et al.* [12]. For each of the nine combinations of concrete strength and groove height-to-width ratio, five values of groove spacing are chosen based on the height of the FRP strip: 0 mm, 20mm, 40mm, 60mm and 80 mm for bond joints with NSM FRP strips with a height of 10mm; 0 mm, 30mm, 60mm, 90mm and 120mm for bond joints with NSM FRP strips with a height of 20mm; and 0 mm, 40mm, 80mm, 120mm and 160mm for bond joints with NSM FRP strips with a height of 30mm. The value of 0mm of the groove spacing refers to the special case in which the two FRP strips are bonded together to form a compound strip whose thickness is twice of the original ones. As shown in Table 1, the name of each numerical case starts with a letter “C”, followed by a letter “f” and a Roman numeral to represent the concrete strength ( $f_c$ ), a letter “h” and a Roman numeral to represent the height of the CFRP strip ( $h_f$ ), and two letters “ag” and a Roman numeral to represent the groove spacing ( $a_g$ ). For instance, Case-f20-h10-ag20 refers to the specimen which has a concrete strength of 20 MPa, a FRP strip height of 10 mm and a groove spacing of 20 mm.

# 5 RESULTS OF PARAMETRIC STUDY

## 5.1 Failure process

The Specimen Case-f20-h10-ag60 is selected as an example to demonstrate the predicted typical failure process of bonded joints with two FRP strips, as shown in Fig. 3, in which the distribution of maximum principal cracking strains in the concrete are plotted. It can be seen from Fig. 3, at the initial stage of loading, only a few cracks develop in a very small region near the loaded end while most of the concrete block is still in the elastic range (Fig. 3a). With the increase of the applied load, the width of cracks becomes larger (identified by the color of the plotted maximum principal cracking strain) and the crack region extends in a stereoscopic manner (Fig. 3b). Transverse cracks (i.e., in the plane perpendicular to the load direction) form in the concrete between the two parallel grooves. These cracks are almost vertical within a small layer of the concrete near the top surface of the specimen and become inclined to the horizontal at an angle of around 45 degree when the depth increases. On the other side of the groove (i.e., outside the region sandwiched by the two grooves), the fish-spine-like cracks (i.e., cracks at around 45 degree to the loading direction) appear on the top surface of the specimen. The discrepancies in the crack patterns on the two sides of the groove reveal that the stress states in the concrete on the two sides of the groove are significantly different from each other. This further indicates that interaction between the two grooves exists during the loading process, which influences the behavior of concrete in between. With the further increase in the applied load, more cracks form and the cracking region gradually propagates along the bondline to the free end of NSM FRP strips (Fig. 3c). At the final stage, the cracking region takes up around 60% of the bond length and does not reach the edge of the concrete block (Fig. 3d), indicating that the bond length and edge distance chosen for the specimen are sufficiently large to prevent their detrimental effects on the bond strength. It can be clearly seen from Fig. 3d that most transverse cracks in the

concrete sandwiched by the two grooves connect with adjacent ones at a depth of the groove height, resulting in a big horizontal crack on the plane passing through the bottom surface of the groove. This horizontal crack means that the concrete sandwiched by the two grooves is pulled out with the two FRP strips, which agree well with the experimental observations made by Rashid *et al.* [24].

## 5.2 Bond strength

As only half of the specimen was included in the FE modelling by taking advantage of symmetry, the bond strength of the whole specimen was obtained by multiplying the ultimate load directly obtained from the FE modelling by 2. The bond strengths obtained from the parametric study are listed in Table 2, and the relationships between the bond strength and groove spacing are plotted in Fig. 4.

It can be seen from Fig. 4 that: (1) a larger concrete strength or a larger height of FRP strip gives a larger bond strength of the specimen, which agrees with the findings for bonded joint with a single FRP strip [13]; (2) the bond strength increases with the value of groove spacing but the increasing rate decreases largely with the value of groove spacing. When the value of groove spacing is larger than a certain value, further increase in the groove spacing gives marginal if not no increase in the bond strength. It can be seen from Table 2 that, for all studied series of numerical specimens, the bond strength of the specimens with the largest value of groove spacing studied in that series is very close to that with the second largest groove spacing, indicating that the value of bond strength has been converged with respect to the value of groove spacing.

## 5.3 Threshold value of groove spacing

In the present study, the minimum required value of groove spacing for the full development of bond strength of the bonded joint with two FRP strips is termed as the threshold value of

285 groove spacing (i.e., $a_{gt}$ in Table 2). The threshold value of groove spacing listed in Table 2
286 are obtained using the following steps: (1) for each of the nine series of the numerical
287 specimens, find the best-fit four-order polynomial function to describe the relationship
288 between the bond strength and the value of groove spacing; (2) use the obtained best-fit
289 four-order polynomial function to calculate the value of groove spacing which corresponds to
290 99% of the bond strength obtained with the largest groove spacing in that series, and this
291 groove spacing value is treated as the threshold value of groove spacing in the present study.
292 The threshold values of groove spacing obtained using this method are listed in Table 2.
293
294 It can be seen from Table 2 that a larger groove height (i.e., a larger FRP height) or a higher
295 concrete strength leads to a larger threshold value of groove spacing, which is not difficult to
296 understand: a deeper groove or a higher strength of concrete usually incurs a larger motivated
297 stress zone around the groove and consequently a larger overlapping zone of the stress for a
298 given value of groove spacing. To find the calculation equation for the threshold value of
299 groove spacing, firstly, the relationship between the threshold value of groove spacing and
300 the groove height is plotted in Fig. 5a, in which the best-fit power functions are also shown. It
301 can be seen from Fig. 5a that the relationship between the threshold value of groove spacing
302 and the groove height can be described by the following power function:
303 $$a_{gt} = A \times h_g^B \quad (1)$$
304 where the coefficient *A* and the power *B* are related to the concrete strength $f_c$. The
305 relationship between the coefficient *A* and the concrete strength is shown in Fig. 5b, and the
306 relationship between the power *B* and the concrete strength is shown in Fig. 5c. Based on the
307 best-fit curves shown in Figs. 5b and 5c, two linear functions are respectively proposed for
308 the coefficient *A* and the power *B*:
309 $$A = 0.046\, f_c + 3.07 \quad (2)$$

$$B = -0.002\, f_c + 1.03 \tag{3}$$

The predictions of the threshold value of groove spacing from Eq. (1) are compared with the results from the FE analysis (see Table 2) in Fig. 5d, from which close agreement can be observed. It can be seen from Table 2 that the ratios between predictions of Eq. (1) and FE analysis have an average value of 1.003, a standard deviation (STD) of 0.024, and a coefficient of variation (CoV) of 0.023.

### 5.4 Reduction factor $\beta_g$ accounting for the effect of groove spacing

As can be seen from the parametric study, when the groove spacing is smaller than the threshold value, interaction between adjacent grooves/FRP strips exists and as a result, the maximum load $\overline{P_u}$ that could be resisted by each FRP strip in bonded joints with multiple FRP strips will be smaller than the bond strength of NSM bonded joints with a single FRP strip $P_u$. To account for this detrimental effect on the bond strength, a reduction factor $\beta_g$ needs to be introduced as

$$\overline{P_u} = \beta_g P_u \tag{4}$$

In the present study, it is assumed that $\overline{P_u}$ is equal to $P_u$ when the groove spacing reaches the threshold value $a_{gt}$. To get $\beta_g$, for each studied series in the parametric study, the threshold value of groove spacing and the corresponding bond strength are treated as the references, with respect to which other groove spacings and bond strengths are normalized respectively. The normalized bond strength versus the normalized groove spacing curves just represent the reduction factor $\beta_g$ and are shown in Fig. 6a, from which it can be seen that although the curves do not perfectly coincide with each other, the scatter is very small. By regressing all the points on Fig. 6a, the following equation is proposed for the reduction factor $\beta_g$:

$$\beta_g = -0.23\left(\frac{a_g}{a_{gt}}\right)^2 + 0.51\left(\frac{a_g}{a_{gt}}\right) + 0.72 \le 1 \quad (5)$$

Although Eq. (5) can give accurate prediction of the reduction factor, its form is relatively complex. Therefore, a simplified reduction factor, described by linear function expressed in Eq. (6), is also proposed and assessed in the present study.

$$\beta_g = 0.72 + 0.28\left(\frac{a_g}{a_{gt}}\right) \le 1 \quad (6)$$

Fig. 6b shows the comparison of predictions given by Eq. (5) and Eq. (6). It can be seen from Fig. 6b that the simplified reduction factor (Eq. 6) is close to and consistently lower than the accurate reduction factor (Eq. 5).

It should be noted that the $\beta_g$ in Eq. (5) or (6) is only applicable for FRP strips in bonded joints with two FRP strips and the two outmost FRP strips in bonded joints with three or more FRP strips (i.e., the detrimental effect caused by an insufficient groove spacing only exists on one side of the FRP strip). For FRP strips suffering the detrimental effect from both sides, such as the inner FRP strips in bonded joints with three or more FRP strips, the reduction factor $\beta_{g\_in}$ can be obtained through the following analysis.

For FRP strips which have adjacent FRP strip on one side but not on the other side, the ultimate load that can be resisted by the FRP strip is given by

$$\overline{P_u} = P_{u1} + P_{u2} \quad (7)$$

Where $P_{u1}$ is the load contributed by the bond from the side in which no adjacent FRP strip exist, and can be assumed to be half of the bond strength of NSM bonded joints with a single FRP strip, i.e., $0.5P_u$; and $P_{u2}$ is the load contributed by the bond from the side in which

adjacent FRP strip exists, and can be expressed as $\beta_{g\_in} \times (0.5P_u)$. Therefore, Eq. (7) can be expressed as

$$\overline{P_u} = 0.5P_u + 0.5\beta_{g\_in}P_u \tag{8}$$

Combining Eqs. (4) and (8) gives:

$$\beta_{g\_in} = 2\beta_g - 1 \tag{9}$$

## 5.5 Bond strength model

Based on the above consideration, the bond strength model for bonded joints with multiple evenly-spaced FRP strips can be expressed as:

$$P_{u\_m} = \left(2\beta_g + \sum_{0}^{n-2}\beta_{g\_in}\right)p_u \tag{10}$$

where *n* is the number of FRP strips; $P_u$ is the bond strength of NSM bonded joints with a single FRP strip and can be obtained using the equation proposed by Zhang *et al.* [13]:

$$P_u = \sqrt{2G_f E_f A_f C_{failure}} \le P_t \quad \text{when} \quad L_b \ge L_e \tag{11}$$

$$P_u = \beta_L\sqrt{2G_f E_f A_f C_{failure}} \le P_t \quad \text{when} \quad L_b < L_e \tag{12}$$

$$G_f = 0.40\gamma^{0.422} f_c^{0.619} \tag{13}$$

$$L_e = \frac{1.66}{\eta} \tag{14}$$

$$\eta^2 = \frac{\tau_{\max}^2 C_{failure}}{2G_f E_f A_f} \tag{15}$$

$$\tau_{\max} = 1.15\gamma^{0.138} f_c^{0.613} \tag{16}$$

$$\beta_L = \frac{L_b}{L_e}(2.08 - 1.08\frac{L_b}{L_e}) \tag{17}$$

where $A_f$ (mm$^2$) is the cross sectional area of a single FRP strip; $C_{failure}$ (mm) is taken to be the sum of the three side lengths of the groove; $E_f$ (MPa) is the elastic modulus of the FRP

strip; $f_c$ (MPa) is the compressive strength of concrete cylinder; $G_f$ (N/mm) is the interfacial fracture energy; $L_b$ (mm) is the bond length; $L_e$ (mm) is the effective bond length; $P_t$ (N) is the full tensile capacity of a single FRP strip; $\tau_{\max}$ (MPa) is the maximum bond stress, $\gamma$ is the groove height-to-width ratio, $\beta_L$ the a reduction factor to consider the detrimental effect of insufficient bond lengths.

# 6 VERIFICATION OF THE PROPOSED BOND STRENGTH MODEL

## 6.1 Comparison with FE results

The comparison of bond strength between the prediction of Eq. (10) and FE results for the 45 numerical specimens (see Table 2) are listed in Table 3 and plotted in Fig. 7. It can be seen from Table 3 that, if the detrimental effect of groove spacing is ignored (i.e., the reduction factor is set to 1.0), the proposed bond strength model overestimates the FE results with an average prediction-to-FE load ratio of 1.142, and the scatter of the prediction is relatively large with a STD of 0.152 and a CoV of 0.133. If the accurate reduction factor (Eq. 5) is adopted, the performance of the proposed bond strength model is largely improved, with the average, STD and CoV of prediction-to-FE load ratio being 1.017, 0.011 and 0.011 respectively. It can be also seen form Table 3 that the proposed bond strength model with the simplified reduction factor (Eq. 6) can give similarly accurate prediction to that with the accurate reduction factor (Eq. 5), with the average, STD and CoV of prediction-to-FE load ratio being 1.008, 0.050 and 0.050 respectively. The better performance of the bond strength model with either the accurate reduction factor or the simplified reduction factor can be also evidenced by the much smaller scatter of the points plotted in Fig. 7: the points predicted by either the accurate reduction factor or the simplified reduction factor are very close to the diagonal line (i.e., y=x), while most points predicted without considering the detrimental effect of groove spacing are far away from the diagonal line.

## 6.2 Comparison with test results

By far, a large number of experimental studies have been conducted on the bond strength of NSM bonded joints [13], but most studies are for bonded joints with a single FRP strip. To the best knowledge of the authors, so far the only experimental study (published in English) on bonded joints with two FRP strips is from Rashid *et al.* [24]. There have been studies on RC flexural members strengthened with multiple NSM FRP strips, such as the tests on RC girders (recovered from a 42-year-old bridge) strengthened with 8 NSM CFRP strips evenly embedded in 4 grooves [25] and the tests on RC beams strengthened with 8 NSM CFRP strips evenly embedded in 4 grooves [26]. However, no experimental study (published in English) on bonded joints with three or more NSM FRP strips was found in the open literature. In Rashid *et al.*'s [24] tests, two parallel CFRP strips with an aspect ratio of 16.7 (i.e., the height of 20mm and the width of 1.2mm) were used in each specimen, with the groove spacing between them being varied to study its effect on the bond strength. Recently, the authors conducted a series of tests on bonded joints with two parallel CFRP strips to study the effect of groove spacing, using the test setup shown in Fig. 8. In the test, the concrete block has a height of 150mm, a length of 400 mm and a width of 300 mm; the CFRP strip had a height of 16mm, a thickness of 2 mm and a bond length of 350mm; the tensile strength and elastic modulus of the CFRP strips, averaged from three tensile specimens, were found to be 2131 MPa and 123 GPa respectively. The details of all specimens are listed in Table 4.

The comparison of the bond strength between the prediction from the proposed model (i.e. Eq. 10) and test results are listed in Table 4 and plotted in Fig. 9. As can be seen from Table 4, if the detrimental effect of groove spacing is ignored, the proposed bond strength model gives an average value, a STD and a CoV of prediction-to-test load ratio of 0.987, 0.103 and 0.104 respectively. If the accurate reduction factor is used to consider such detrimental effect, the

performance of the proposed bond strength model is improved as the STD and CoV of prediction-to-test load ratio are reduced to 0.062 and 0.070 respectively. The smaller average prediction-to-test load ratio of 0.889 obtained with the accurate reduction factor does not mean the poor performance of the reduction factor model, in the sense that (1) the smaller average prediction-to-test load ratio is caused by $P_u$, which was proposed to give a conservative prediction of the test results (see Zhang *et al.* [13]); (2) the average value can be easily increased by introducing an amplifying coefficient into the bond strength model, without influencing the values of STD and CoV which are the more reasonable statistical characteristics to judge the performance of the proposed reduction factor models. Compared with the accurate reduction factor (Eq. 5), the simplified reduction factor (Eq. 6) leads to nearly the same STD and CoV values of prediction-to-test load ratio (0.059 and 0.070 respectively), but a slightly smaller average prediction-to-test load ratio of 0.845. The smaller average value of prediction-to-test load ratio is because that the reduction factor predicted by the simplified model (Eq. 5) is always smaller than that by the accurate model (Eq. 6), as shown in Fig. 6. The better performance of the proposed bond strength models with either the accurate reduction factor or simplified reduction factor can be also seen from the smaller scatter of the points and the smaller R-squared values shown in Fig. 9. The above comparison indicates that the proposed model can provide reasonably accurate and conservative predictions of the test results.

## 7 CONCLUDING REMARKS

This paper has been concerned with the adverse effect of groove spacing (i.e., the net distance between grooves) on the bond strength of NSM bonded joints with multiple FRP strips. A 3-D meso-scale FE model for NSM bonded joints with two FPP strips separately embedded in two parallel grooves is first established, based on the FE model previously developed by

449 the author [14] for NSM bonded joints with a single FRP strip. The developed FE model is
450 then employed in a numerical parametric study to investigate the reduction of the bond
451 strength of each NSM FRP strip caused by the adverse effect from the adjacent groove. Based
452 on the results from the numerical parametric study, the equation for the threshold value of
453 groove spacing (i.e., the minimum required value of groove spacing for the full development
454 of bond strength of the bonded joint with two FRP strips) is formulated, and the bond strength
455 model for NSM bonded joints with multiple FRP strips is proposed with two reduction
456 factors (an accurate reduction factor and a simplified reduction factor) accounting for the
457 adverse effect of groove spacing being introduced. Based on the findings in the present study,
458 the following conclusions can be drawn:

459 (1) The bond strength of each NSM FRP strip in bonded joints with multiple FRP strips can
460 be significantly influenced by the adjacent groove/FRP strip, when the groove spacing is
461 relatively small. When the groove spacing is larger than a threshold value, such
462 detrimental effect on the bond strength does not exist anymore;

463 (2) For the parametric combinations studied herein, the threshold value of groove spacing is
464 found to be mainly dependent on the groove height and the concrete strength. In general,
465 a larger groove height or concrete strength leads to a larger threshold value; and

466 (3) Comparison of the bond strength between existing FE/test results and predictions of the
467 proposed bond strength model verifies the accuracy of the proposed bond strength model
468 for NSM bonded joints with two FRP strips. More experimental studies, especially on
469 NSM bonded joints with three/more FRP strips, are still in a need for the further
470 verification the proposed model.

## ACKNOWLEDGEMENTS

The authors would like to acknowledge the financial support provided by the Australian Government through the Australian Research Council's *Discovery Projects* funding scheme (project ID: DP170102992).

## REFERENCES

[1]. De Lorenzis, L. and Teng, J.G. (2007). "Near-surface mounted FRP reinforcement: an emerging technique for strengthening structures." *Composites-Part B: Engineering*, 38(2), 119-143.

[2]. Perera, W. K. K. G., Ibell, T. J., and Darby, A. P. (2013). "Bond characteristics of near surface mounted CFRP bars." *Construction and Building Materials*, 43, 58-68.

[3]. Lee, D., Cheng, L.J., Hui, J.Y.G. (2013). "Bond characteristics of various NSM FRP reinforcements in concrete." *Journal of Composites for Construction*, ASCE, 17(1), 117-129.

[4]. Bilotta, A., Ceroni, F., Nigro, E. and Pecce, M. (2014). "Strain assessment for the design of NSM FRP systems for the strengthening of RC members." *Construction and Building Materials*, 69, 143-158.

[5]. Coelho, M.R.F., Sena-Cruz, J.M., Neves, L.A.C. (2015). "A review on the bond behavior of FRP NSM systems in concrete." *Construction and Building Materials*, 93, 1157-1169.

[6]. Barros, J.A.O., Costa, I.G. and Ventura-Gouveia, A. (2011). "CFRP Flexural and Shear Strengthening Technique for RC Beams: Experimental and Numerical Research." *Advances in Structural Engineering*, 14(3), 551-573.

[7]. Zhang, S.S., Yu, T., and Chen, G.M. (2017). "Reinforced concrete beams strengthened in flexure with near-surface mounted (NSM) CFRP strips: current status and research

needs.” *Composites Part B: Engineering*, under review.

[8]. Chen, J.F. and Teng, J.G. (2001). “Anchorage strength models for FRP and steel plates bonded to concrete.” *Journal of Structural Engineering*, ASCE, 127(7), 784-791.

[9]. Seracino, R., Jones, N.M., Ali, M.S.M., Page, M.W., and Oehlers, D.J. (2007). “Bond strength of near-surface mounted FRP strip-to-concrete joints.” *Journal of Composites for Construction*, ASCE, 11(4), 401-409

[10]. Seracino, R., Saifulnaz, M.R.R., and Oehlers, D.J. (2007). “Generic debonding resistance of EB and NSM plate-to-concrete joints.” *Journal of Composites for Construction*, ASCE, 11(1), 62-70.

[11]. Sena Cruz, J.M., and Barros, J.A.O. (2004). “Bond between near-surface mounted carbon-fiber-reinforced polymer laminate strips and concrete.” *Journal of Composites for Construction*, ASCE, 8(6), 519-527.

[12]. Zhang, S.S., Teng, J.G. and Yu, T. (2013). “Bond-slip model for CFRP strips near-surface mounted to concrete”, *Engineering Structures*, 56, 945-953.

[13]. Zhang, S.S., Teng, J.G., and Yu, T. (2014). “Bond strength model for CFRP strips near-surface mounted to concrete.” *Journal of Composites for Construction*, ASCE, 18(3), Article Number: A4014003. doi: 10.1061/(asce)cc.1943-5614.0000402.

[14]. Teng, J.G., Zhang, S.S., Dai, J.G. and Chen, J.F. (2013). “Three-dimensional meso-scale finite element modeling of bonded joints between a near-surface mounted FRP strip and concrete.” *Computers and Structures*, 117, 105–117.

[15]. MSC.MARC (2005). *User's Manual. MSC. Software Corporation*, 2 MacArthur Place, Santa Ana, California 92707, USA.

[16]. Bazant, Z. P. and Oh, B. H. (1983). “Crack band theory for fracture of concrete.” *Materials and Structures*, 16(93), 155-177.

[17]. CEB-FIP. (1990). *Model Code 90*, Lausanne, Switzerland, 1993

[18]. Buyukozturk, O. (1977). “Nonlinear analysis of reinforced concrete structures.” *Computers and Structures*, 7, 149-156.

[19]. Elwi, A. A. and Murray, D. W. (1979). “A 3D hypoelastic concrete constitutive relationship.” *Journal of the Engineering Mechanics Division*, ASCE, 105(4), 623-641.

[20]. Hordijk, D. A. (1991). *Local Approach to Fatigue of Concrete*, PhD thesis, Delft University of Technology, 1991.

[21]. Okamura, H. and Maekawa, K. (1991). *Nonlinear Analysis and Constitutive Models of Reinforced Concrete*, Tokyo: Gihodo-Shuppan.

[22]. Zhang, S.S. and Teng, J.G. (2014). “Finite element analysis of end cover separation in RC beams strengthened in flexure with FRP”, *Engineering Structures*, 75, 550-560.

[23]. Zhang, S.S. and Teng, J.G. (2015). “End cover separation in RC beams strengthened in flexure with bonded FRP reinforcement: simplified finite element approach”, *Materials and Structures*, 49 (6), 2223-2236.

[24]. Rashid, R., Oehlers, D.J., and Seracino, R. (2008). “IC debonding of FRP NSM and EB retrofitted concrete: plate and cover interaction tests.” *Journal of Composites for Construction*, ASCE, 12(2), 160-167.

[25]. Aidoo, J., Harries, K. A. and Petrou, M. F. (2006). “Full-scale experimental investigation of repair of reinforced concrete interstate bridge using CFRP materials,” *Journal of Bridge Engineering*, ASCE, 11(3), 350-358.

[26]. Rasheed, H. A., Harrison, R. R., Peterman, R. J. and Alkhrdaji, T. (2010). “Ductile Strengthening Using Externally Bonded and Near Surface Mounted Composite Systems,” *Composite Structures*, 92 (10), 2379-2390.

## TABLES

Table 1 Design of parametric study of groove spacing

| Specimens | $f_c$ (MPa) | $t_f$ (mm) | $h_f$ (mm) | $E_f$ (GPa) | $h_f / t_f$ | $a_e$ (mm) | $a_g$ (mm) |
|---|---|---|---|---|---|---|---|
| Case-f20-h10-ag0, 20,40, 60 or 80 | 20 | 2 | 10 | 150 | 5 | 60 | 0, 20, 40, 60 and 80 |
| Case-f20-h20-ag0, 30, 60, 90, or 120 | 20 | 2 | 20 | 150 | 10 | 100 | 0, 30, 60, 90, and 120 |
| Case-f20-h30-ag0, 40, 80, 120 or 160 | 20 | 2 | 30 | 150 | 15 | 140 | 0, 40, 80, 120 and 160 |
| Case-f30-h10-ag0, 20,40, 60 or 80 | 30 | 2 | 10 | 150 | 5 | 60 | 0, 20, 40, 60 and 80 |
| Case-f30-h20-ag0, 30, 60, 90, or 120 | 30 | 2 | 20 | 150 | 10 | 100 | 0, 30, 60, 90, and 120 |
| Case-f30-h30-ag0, 40, 80, 120 or 160 | 30 | 2 | 30 | 150 | 15 | 140 | 0, 40, 80, 120 and 160 |
| Case-f40-h10-ag0, 20,40, 60 or 80 | 40 | 2 | 10 | 150 | 5 | 60 | 0, 20, 40, 60 and 80 |
| Case-f40-h20-ag0, 30, 60, 90, or 120 | 40 | 2 | 20 | 150 | 10 | 100 | 0, 30, 60, 90, and 120 |
| Case-f40-h30-ag0, 40, 80, 120 or 160 | 40 | 2 | 30 | 150 | 15 | 140 | 0, 40, 80, 120 and 160 |

Table 2 Threshold values of groove spacing

| Specimens | Bond strength (kN) with different $a_g$ (mm) | | | | | $a_{gt}$ (mm) | | |
|---|---|---|---|---|---|---|---|---|
| | 0mm | 20mm | 40mm | 60mm | 80mm | FE analysis | Prediction of Eq. (1) | Prediction / FE analysis |
| Case-f20-h10-ag0, 20,40, 60 or 80 | 38.23 | 46.68 | 51.94 | 53.29 | 53.71 | 53.4 | 54.4 | 1.020 |
| Case-f30-h10-ag0, 20,40, 60 or 80 | 43.86 | 53.29 | 58.91 | 61.13 | 61.59 | 57.2 | 57.6 | 1.006 |
| Case-f40-h10-ag0, 20,40, 60 or 80 | 48.34 | 58.79 | 64.94 | 67.28 | 67.91 | 59.1 | 60.2 | 1.020 |
| Specimens | Bond strength (kN) with different $a_g$ (mm) | | | | | $a_{gt}$ (mm) | | |
| | 0mm | 30mm | 60mm | 90mm | 120mm | | | |
| Case-f20-h20-ag0, 30, 60, 90, or 120 | 76.04 | 90.75 | 100.24 | 105.21 | 106.75 | 95.1 | 92.8 | 0.975 |
| Case-f30-h20-ag0, 30, 60, 90, or 120 | 87.20 | 105.00 | 115.59 | 120.57 | 122.71 | 100.8 | 97.1 | 0.964 |
| Case-f40-h20-ag0, 30, 60, 90, or 120 | 96.11 | 114.04 | 126.01 | 132.08 | 134.78 | 103.0 | 100.5 | 0.976 |
| Specimens | Bond strength (kN) with different $a_g$ (mm) | | | | | $a_{gt}$ (mm) | | |
| | 0mm | 40mm | 80mm | 120mm | 160mm | | | |
| Case-f20-h30-ag0, 40, 80, 120 or 160 | 116.94 | 139.00 | 154.39 | 162.28 | 164.68 | 127.4 | 131.0 | 1.028 |
| Case-f30-h30-ag0, 40, 80, 120 or 160 | 134.18 | 157.61 | 175.21 | 185.05 | 188.79 | 134.4 | 136.1 | 1.013 |
| Case-f40-h30-ag0, 40, 80, 120 or 160 | 147.89 | 173.97 | 192.55 | 203.44 | 207.98 | 136.1 | 140.0 | 1.028 |
| | | | | | | | **Average =** | 1.003 |
| | | | | | | **Statistical characteristics** | **STD =** | 0.024 |
| | | | | | | | **CoV =** | 0.023 |

Table 3. Bond strength comparison between predictions and FE results

| | $t_f$ (mm) | $h_f$ (mm) | $w_g$ (mm) | $h_g$ (mm) | $E_f$ (GPa) | $a_g$ (mm) | $f_c$ (MPa) | FE (kN) | Without reduction factor | | With reduction factor given by Eq. (5) | | With reduction factor given by Eq. (6) | |
|---|---|---|---|---|---|---|---|---|---|---|---|---|---|---|
| | | | | | | | | | Prediction (kN) | Prediction / FE | Prediction (kN) | Prediction / FE | Prediction (kN) | Prediction / FE |
| Case-f20-h10-ag0 | 2 | 10 | 6 | 14 | 150 | 0 | 20 | 38.23 | 54.6 | 1.428 | 39.3 | 1.028 | 39.3 | 1.028 |
| Case-f20-h10-ag20 | 2 | 10 | 6 | 14 | 150 | 20 | 20 | 46.68 | 54.6 | 1.170 | 47.9 | 1.025 | 44.9 | 0.963 |
| Case-f20-h10-ag40 | 2 | 10 | 6 | 14 | 150 | 40 | 20 | 51.94 | 54.6 | 1.051 | 53.0 | 1.020 | 50.6 | 0.973 |
| Case-f20-h10-ag60 | 2 | 10 | 6 | 14 | 150 | 60 | 20 | 53.29 | 54.6 | 1.024 | 54.6 | 1.024 | 56.2 | 1.054 |
| Case-f20-h10-ag80 | 2 | 10 | 6 | 14 | 150 | 80 | 20 | 53.71 | 54.6 | 1.017 | 54.6 | 1.017 | 61.8 | 1.151 |
| Case-f20-h20-ag0 | 2 | 20 | 6 | 24 | 150 | 0 | 20 | 76.04 | 109.0 | 1.434 | 78.5 | 1.032 | 78.5 | 1.032 |
| Case-f20-h20-ag30 | 2 | 20 | 6 | 24 | 150 | 30 | 20 | 90.75 | 109.0 | 1.201 | 93.9 | 1.034 | 88.4 | 0.974 |
| Case-f20-h20-ag60 | 2 | 20 | 6 | 24 | 150 | 60 | 20 | 100.24 | 109.0 | 1.088 | 104.0 | 1.037 | 98.2 | 0.980 |
| Case-f20-h20-ag90 | 2 | 20 | 6 | 24 | 150 | 90 | 20 | 105.21 | 109.0 | 1.036 | 108.8 | 1.035 | 108.1 | 1.028 |
| Case-f20-h20-ag120 | 2 | 20 | 6 | 24 | 150 | 120 | 20 | 106.75 | 109.0 | 1.021 | 109.0 | 1.021 | 118.0 | 1.105 |
| Case-f20-h30-ag0 | 2 | 30 | 6 | 34 | 150 | 0 | 20 | 116.94 | 168.2 | 1.439 | 121.1 | 1.036 | 121.1 | 1.036 |
| Case-f20-h30-ag40 | 2 | 30 | 6 | 34 | 150 | 40 | 20 | 139.00 | 168.2 | 1.210 | 143.7 | 1.034 | 135.5 | 0.975 |
| Case-f20-h30-ag80 | 2 | 30 | 6 | 34 | 150 | 80 | 20 | 154.39 | 168.2 | 1.090 | 159.1 | 1.031 | 149.9 | 0.971 |
| Case-f20-h30-ag120 | 2 | 30 | 6 | 34 | 150 | 120 | 20 | 162.28 | 168.2 | 1.037 | 167.3 | 1.031 | 164.3 | 1.012 |
| Case-f20-h30-ag160 | 2 | 30 | 6 | 34 | 150 | 160 | 20 | 164.68 | 168.2 | 1.022 | 168.2 | 1.022 | 178.7 | 1.085 |
| Case-f30-h10-ag0 | 2 | 10 | 6 | 14 | 150 | 0 | 30 | 43.86 | 61.9 | 1.411 | 44.6 | 1.016 | 44.6 | 1.016 |
| Case-f30-h10-ag20 | 2 | 10 | 6 | 14 | 150 | 20 | 30 | 53.29 | 61.9 | 1.162 | 53.8 | 1.010 | 50.6 | 0.949 |
| Case-f30-h10-ag40 | 2 | 10 | 6 | 14 | 150 | 40 | 30 | 58.91 | 61.9 | 1.051 | 59.6 | 1.012 | 56.6 | 0.961 |
| Case-f30-h10-ag60 | 2 | 10 | 6 | 14 | 150 | 60 | 30 | 61.13 | 61.9 | 1.013 | 61.9 | 1.013 | 62.6 | 1.025 |
| Case-f30-h10-ag80 | 2 | 10 | 6 | 14 | 150 | 80 | 30 | 61.59 | 61.9 | 1.005 | 61.9 | 1.005 | 68.7 | 1.115 |
| Case-f30-h20-ag0 | 2 | 20 | 6 | 24 | 150 | 0 | 30 | 87.20 | 123.6 | 1.418 | 89.0 | 1.021 | 89.0 | 1.021 |
| Case-f30-h20-ag30 | 2 | 20 | 6 | 24 | 150 | 30 | 30 | 105.00 | 123.6 | 1.177 | 105.8 | 1.007 | 99.7 | 0.949 |
| Case-f30-h20-ag60 | 2 | 20 | 6 | 24 | 150 | 60 | 30 | 115.59 | 123.6 | 1.069 | 117.1 | 1.013 | 110.4 | 0.955 |
| Case-f30-h20-ag90 | 2 | 20 | 6 | 24 | 150 | 90 | 30 | 120.57 | 123.6 | 1.025 | 123.0 | 1.020 | 121.1 | 1.004 |
| Case-f30-h20-ag120 | 2 | 20 | 6 | 24 | 150 | 120 | 30 | 122.71 | 123.6 | 1.007 | 123.6 | 1.007 | 131.8 | 1.074 |
| Case-f30-h30-ag0 | 2 | 30 | 6 | 34 | 150 | 0 | 30 | 134.18 | 190.7 | 1.421 | 137.3 | 1.023 | 137.3 | 1.023 |

| | | | | | | | | | | | | | | |
|---|---|---|---|---|---|---|---|---|---|---|---|---|---|---|
| Case-f30-h30-ag40 | 2 | 30 | 6 | 34 | 150 | 40 | 30 | 157.61 | 190.7 | 1.210 | 162.1 | 1.029 | 153.0 | 0.971 |
| Case-f30-h30-ag80 | 2 | 30 | 6 | 34 | 150 | 80 | 30 | 175.21 | 190.7 | 1.089 | 179.3 | 1.024 | 168.7 | 0.963 |
| Case-f30-h30-ag120 | 2 | 30 | 6 | 34 | 150 | 120 | 30 | 185.05 | 190.7 | 1.031 | 189.0 | 1.021 | 184.4 | 0.997 |
| Case-f30-h30-ag160 | 2 | 30 | 6 | 34 | 150 | 160 | 30 | 188.79 | 190.7 | 1.010 | 190.7 | 1.010 | 200.1 | 1.060 |
| Case-f40-h10-ag0 | 2 | 10 | 6 | 14 | 150 | 0 | 40 | 48.34 | 67.7 | 1.400 | 48.7 | 1.008 | 48.7 | 1.008 |
| Case-f40-h10-ag20 | 2 | 10 | 6 | 14 | 150 | 20 | 40 | 58.79 | 67.7 | 1.151 | 58.5 | 0.994 | 55.0 | 0.936 |
| Case-f40-h10-ag40 | 2 | 10 | 6 | 14 | 150 | 40 | 40 | 64.94 | 67.7 | 1.042 | 64.8 | 0.997 | 61.3 | 0.944 |
| Case-f40-h10-ag60 | 2 | 10 | 6 | 14 | 150 | 60 | 40 | 67.28 | 67.7 | 1.006 | 67.6 | 1.006 | 67.6 | 1.005 |
| Case-f40-h10-ag80 | 2 | 10 | 6 | 14 | 150 | 80 | 40 | 67.91 | 67.7 | 0.996 | 67.7 | 0.996 | 73.9 | 1.088 |
| Case-f40-h20-ag0 | 2 | 20 | 6 | 24 | 150 | 0 | 40 | 96.11 | 135.1 | 1.406 | 97.3 | 1.012 | 97.3 | 1.012 |
| Case-f40-h20-ag30 | 2 | 20 | 6 | 24 | 150 | 30 | 40 | 114.04 | 135.1 | 1.185 | 115.1 | 1.009 | 108.6 | 0.952 |
| Case-f40-h20-ag60 | 2 | 20 | 6 | 24 | 150 | 60 | 40 | 126.01 | 135.1 | 1.072 | 127.3 | 1.011 | 119.9 | 0.951 |
| Case-f40-h20-ag90 | 2 | 20 | 6 | 24 | 150 | 90 | 40 | 132.08 | 135.1 | 1.023 | 134.1 | 1.015 | 131.2 | 0.993 |
| Case-f40-h20-ag120 | 2 | 20 | 6 | 24 | 150 | 120 | 40 | 134.78 | 135.1 | 1.003 | 135.1 | 1.003 | 142.4 | 1.057 |
| Case-f40-h30-ag0 | 2 | 30 | 6 | 34 | 150 | 0 | 40 | 147.89 | 208.5 | 1.410 | 150.1 | 1.015 | 150.1 | 1.015 |
| Case-f40-h30-ag40 | 2 | 30 | 6 | 34 | 150 | 40 | 40 | 173.97 | 208.5 | 1.198 | 176.6 | 1.015 | 166.8 | 0.959 |
| Case-f40-h30-ag80 | 2 | 30 | 6 | 34 | 150 | 80 | 40 | 192.55 | 208.5 | 1.083 | 195.2 | 1.014 | 183.5 | 0.953 |
| Case-f40-h30-ag120 | 2 | 30 | 6 | 34 | 150 | 120 | 40 | 203.44 | 208.5 | 1.025 | 206.0 | 1.013 | 200.2 | 0.984 |
| Case-f40-h30-ag160 | 2 | 30 | 6 | 34 | 150 | 160 | 40 | 207.98 | 208.5 | 1.002 | 208.5 | 1.002 | 216.9 | 1.043 |
| | | | | | | | | | **Average =** | 1.142 | | 1.017 | | 1.008 |
| | | | | | | | | **Statistical characteristics** | **STD =** | 0.152 | | 0.011 | | 0.050 |
| | | | | | | | | | **CoV =** | 0.133 | | 0.011 | | 0.050 |

Table 4. Bond strength comparison between predictions and test results

| | Specimen | $t_f$ (mm) | $h_f$ (mm) | $w_g$ (mm) | $h_g$ (mm) | $E_f$ (GPa) | $a_g$ (mm) | $f_c$ (MPa) | Test (kN) | Without reduction factor | | With reduction factor given by Eq. (5) | | With reduction factor given by Eq. (6) | |
|---|---|---|---|---|---|---|---|---|---|---|---|---|---|---|---|
| | | | | | | | | | | Prediction (kN) | Prediction / FE | Prediction (kN) | Prediction / FE | Prediction (kN) | Prediction / FE |
| Rashid et al. (2008) | G30NSM | 1.2 | 20 | 3 | 22 | 161 | 30 | 20 | 102.3 | 110.8 | 1.083 | 90.0 | 0.880 | 90.0 | 0.880 |
| | G40NSM | 1.2 | 20 | 3 | 22 | 161 | 40 | 20 | 124.3 | 110.8 | 0.891 | 99.7 | 0.802 | 93.4 | 0.751 |
| | G50NSM | 1.2 | 20 | 3 | 22 | 161 | 50 | 40 | 118.5 | 110.8 | 0.935 | 103.1 | 0.870 | 96.8 | 0.817 |
| | G70NSM | 1.2 | 20 | 3 | 22 | 161 | 70 | 40 | 135.5 | 110.8 | 0.818 | 108.1 | 0.798 | 103.6 | 0.765 |
| Tests by the authors | S-30-27 | 2 | 16 | 6 | 20 | 123 | 27 | 32 | 82.5 | 90.9 | 1.102 | 78.4 | 0.951 | 73.8 | 0.895 |
| | S-30-54 | 2 | 16 | 6 | 20 | 123 | 54 | 32 | 98.2 | 90.9 | 0.926 | 86.9 | 0.885 | 82.2 | 0.837 |
| | S-50-27 | 2 | 16 | 6 | 20 | 123 | 27 | 58 | 97.9 | 109.2 | 1.115 | 93.2 | 0.952 | 87.9 | 0.898 |
| | S-50-54 | 2 | 16 | 6 | 20 | 123 | 54 | 58 | 106 | 109.2 | 1.030 | 103.2 | 0.973 | 97.2 | 0.917 |
| | | | | | | | | | **Average =** | 0.987 | | 0.889 | | 0.845 | |
| | | | | | | | | | **STD =** | 0.103 | | 0.062 | | 0.059 | |
| | | | | | | | | | **CoV =** | 0.104 | | 0.070 | | 0.070 | |

**Statistical characteristics**

## FIGURES

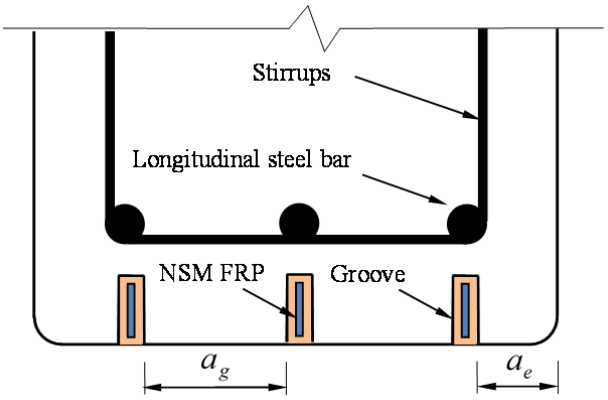


(a) Flexural strengthening

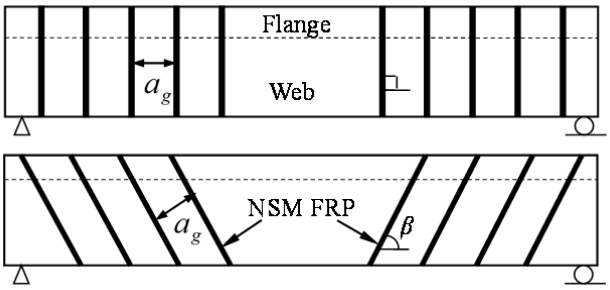


(b) Shear strengthening

Figure 1. Strengthening of RC beams using NSM FRP method

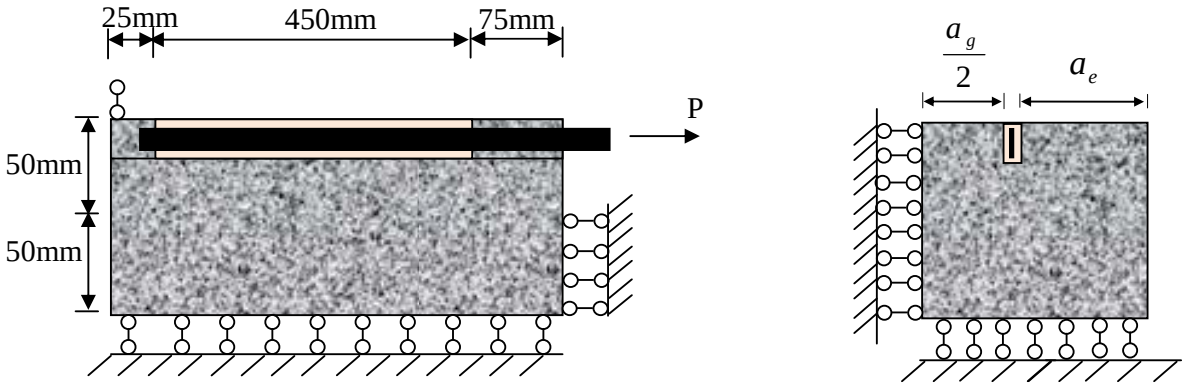


Figure 2. Schematic of the NSM bond joint in parametric studies of the groove spacing

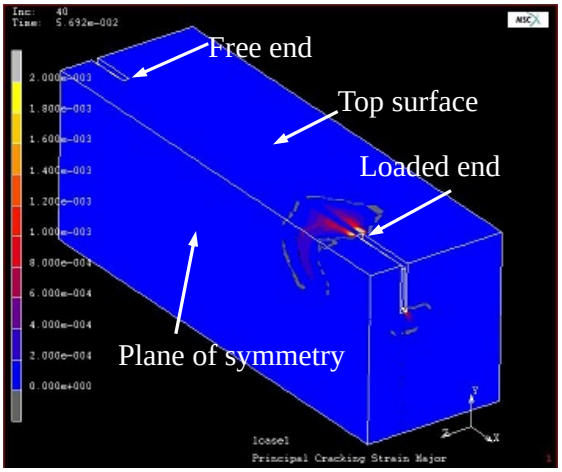


(a)

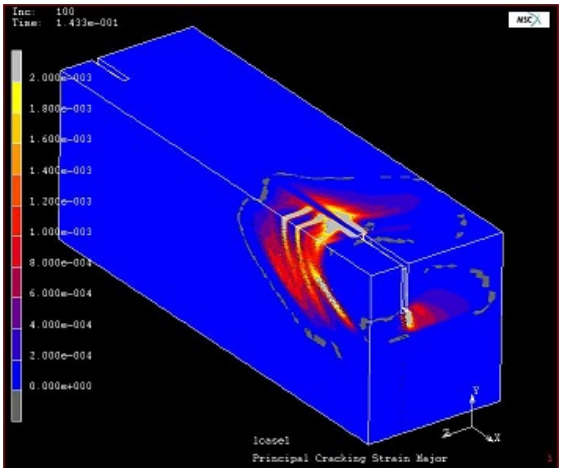


(b)

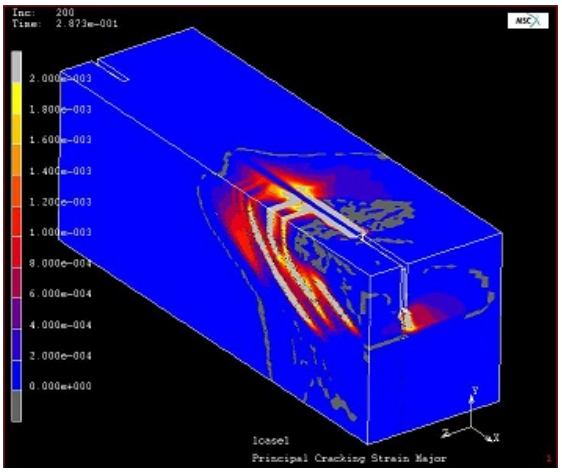


(c)

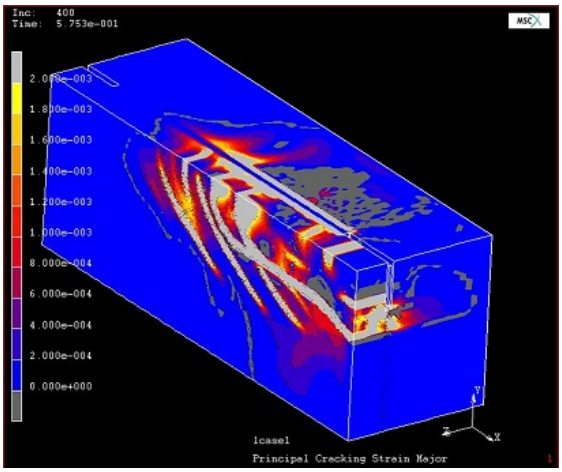


(d)

Figure 3. Failure process

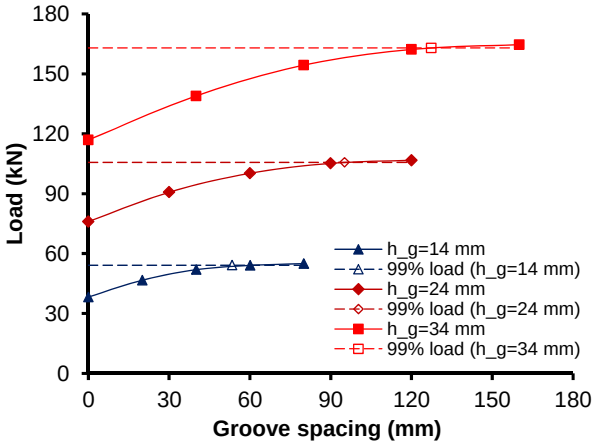


a) $f_c$=20 MPa

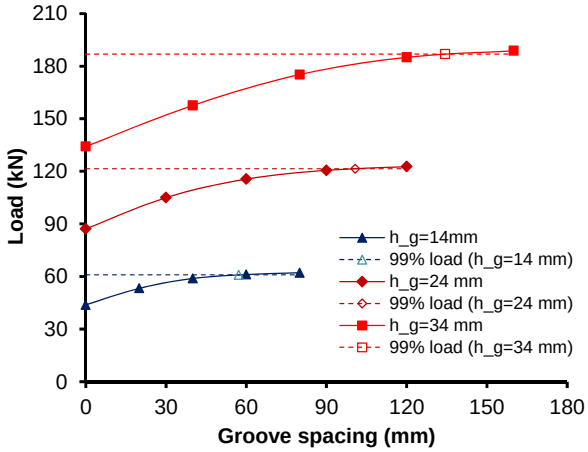


b) $f_c$ =30 MPa

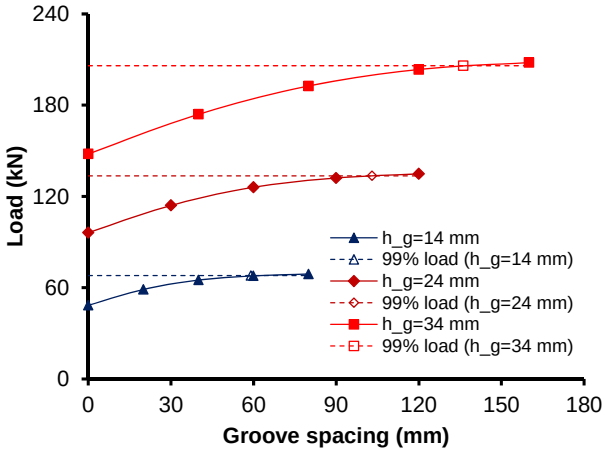


c) $f_c$ =40 MPa

Figure 4. Load versus groove spacing curves

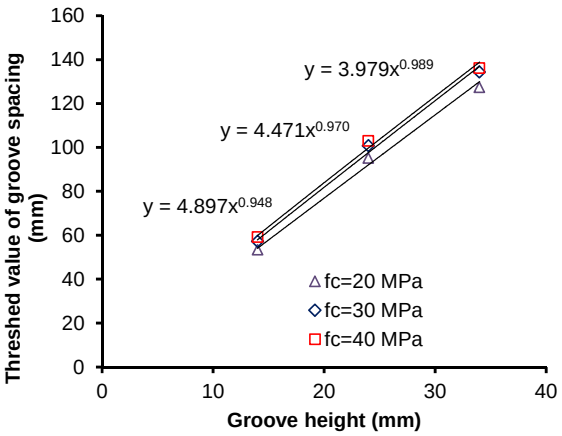


(a) Threshold value versus groove height

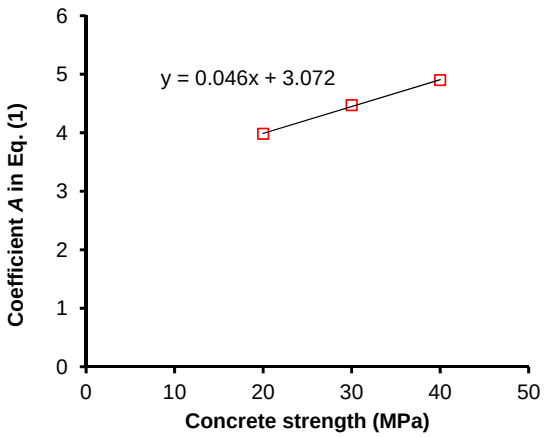


(b) Coefficient A in Eq. (1)

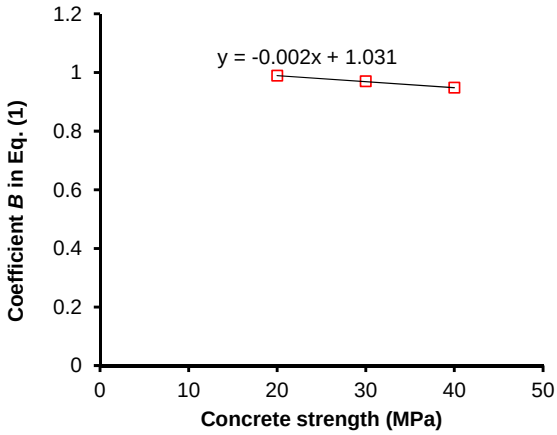


(c) Coefficient B in Eq. (1)

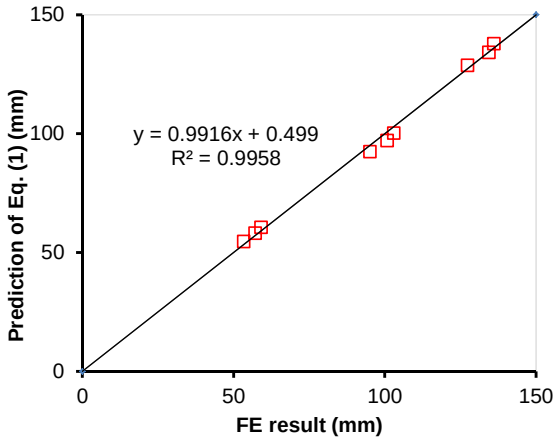


(d) verification of Eq. (1)

Figure 5. The threshold value of groove spacing

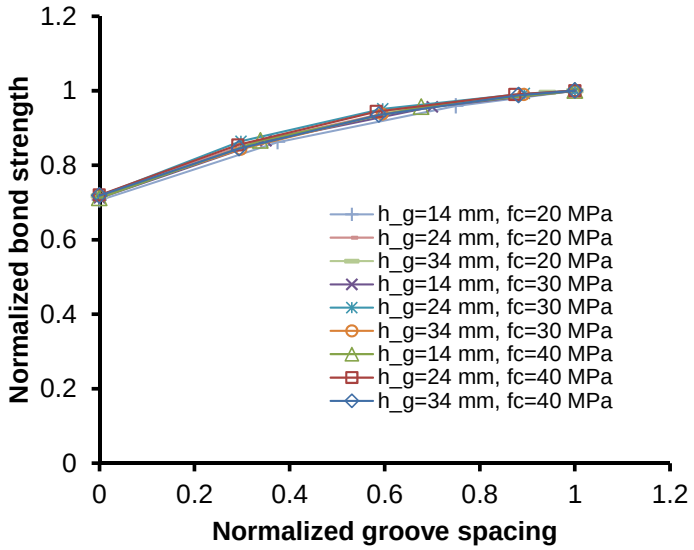


(a) Normalized bond strength versus normalized groove spacing

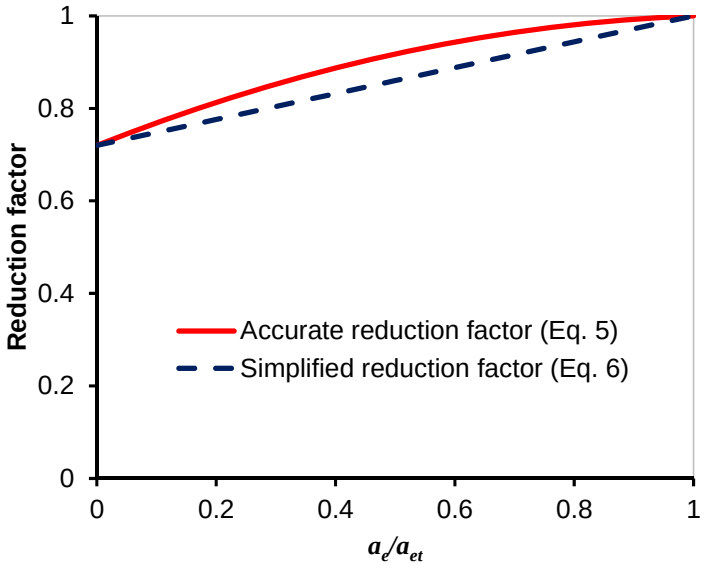


(b) Comparison of the two reduction factor models

Figure 6. Proposed reduction factors: (a) Normalized bond strength versus normalized groove spacing; (b) Comparison of the two reduction factor models

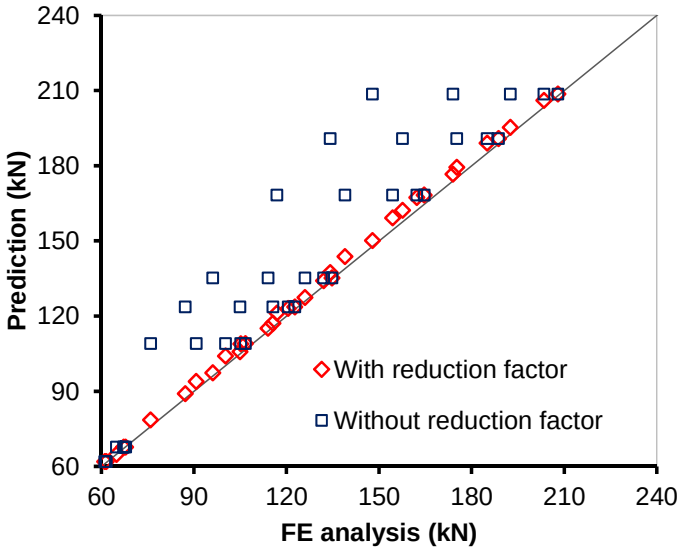


(a) Prediction using the accurate reduction factor (Eq. 5)

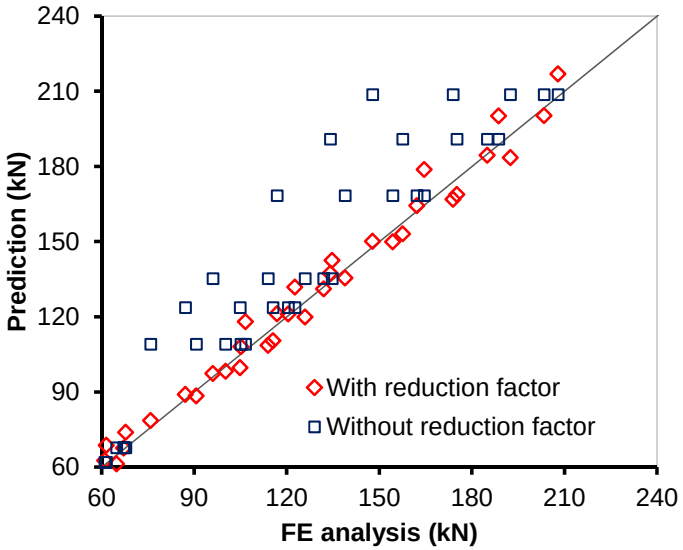


(b) Prediction using the simplified reduction factor (Eq. 6)

Figure 7. Comparison of bond strength between predictions and FE results: (a) Prediction using the accurate reduction factor (Eq. 5); (b) Prediction using the simplified reduction factor (Eq. 6)


(a) test setup (b) side view (c) front view

Figure 8. Test setup used by the authors

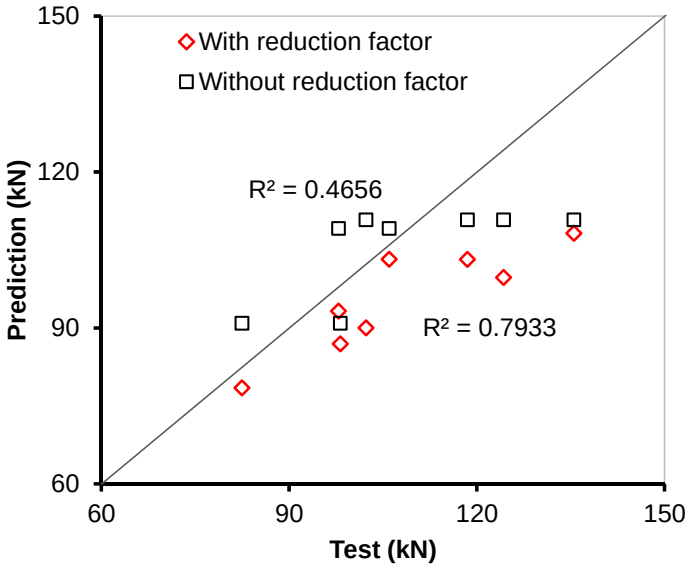


(a) Prediction using the accurate reduction factor (Eq. 5)

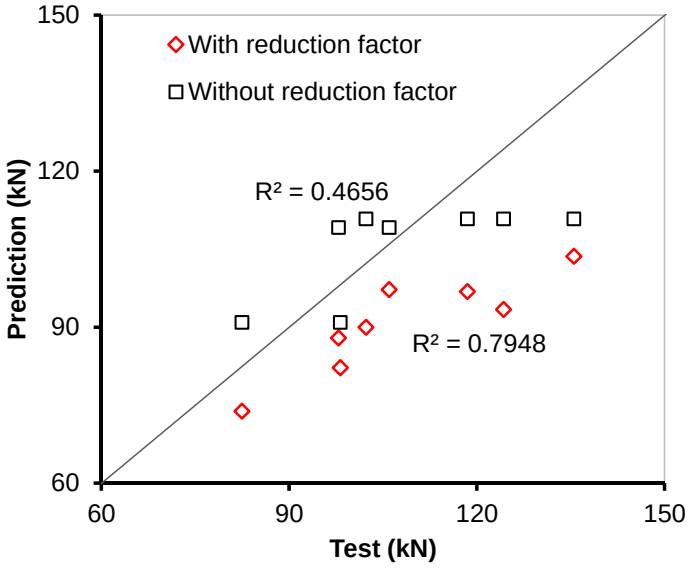


(b) Prediction using the simplified reduction factor (Eq. 6)

Figure 9. Comparison of bond strength between predictions and test results: (a) Prediction using the accurate reduction factor (Eq. 5); (b) Prediction using the simplified reduction factor (Eq. 6)